JOURNAL OF COMPUTATIONAL PHYSICS 39, 226–232 (1981)

Note

Plasma Simulations Using Inversion Symmetry as a Boundary Condition

I. Introduction

Simulation of micro-instabilities in inhomogeneous plasmas is of great current interest. Slab models, which we consider here, have been very useful in dealing with these instabilities [1–4]. Simulation volumes that are often much smaller than typical experimental plasmas have been employed, due to economic and hardware constraints, i.e., the ratio of the length of the simulation volume to characteristic plasma lengths, such as the Debye length or a gyroradius, is not a very large number. Hence, it is tempting to view the simulation volume as a small part of a larger plasma. When this viewpoint is adopted it is necessary that the boundary conditions used, both in advancing the particles or fluid elements and in solving for the fields, reflect the presence of the plasma beyond the simulation boundaries.

In this paper we report on the use of inversion symmetry to obtain such a plasma–plasma boundary, as opposed to a plasma–wall boundary [5, 6]. The use of the inversion symmetry as a boundary condition was originally motivated by the physics of drift waves in an inhomogeneous plasma. In a slab plasma, as shown in Fig. 1, for example, the electron drift waves propagate up (perpendicular to both magnetic field and density gradient) in the region $x > 0$ and down in the region $x < 0$; similar phenomena occur in these two regions except that they are inversion symmetric. This allows us to study the phenomenon by simulating only the half of the slab, say, $x > 0$, reducing the computation by a factor of 2. The allowed perturbations, which must be even under inversion, include many important instabilities, e.g., electron drift waves, drift cyclotron instability, drift cyclotron loss cone instability and lower hybrid drift instability. We have implemented this boundary in two-dimensional particle simulations, and found it to be a useful alternative to the conducting wall type of boundary used by other workers [5, 6].

II. The Use of Symmetries in Obtaining Boundary Conditions

Let the simulation volume be embedded in a larger plasma. The boundary conditions on the simulation volume may be obtained by demanding that the larger plasma be invariant under an appropriate group of symmetry operations.

The imposition of a symmetry on the larger plasma restricts both the equilibrium and the perturbations that are accessible in the simulation. Hence, it is important to

0021-9991/81/010226-07$02.00/0

Copyright © 1981 by Academic Press, Inc.
All rights of reproduction in any form reserved.

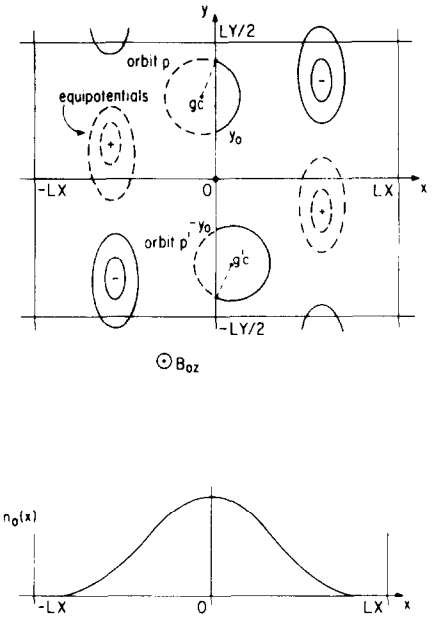

FIG. 1. A two-dimensional model with an inversion symmetry boundary at $x = 0$. The simulation volume is in $0 \leqslant x \leqslant LX$ and $-LY/2 \leqslant y \leqslant LY/2$. The y-axis corresponds to a plasma–plasma boundary. The system has inversion symmetry through the origin $(0, 0)$, has an open boundary at $x = LX$, and is periodic in y. Equilibrium density, $n_0(x)$, is symmetric about $x = 0$.

impose symmetries that are appropriate to the problem at hand. Use of periodic boundaries is appropriate when the larger plasma is uniform in the direction of translation. We therefore choose to impose translational symmetry in the homogeneous coordinate, y, of our plasma slab, yielding periodic boundaries at $y = \pm LY/2$. See Fig. 1.

The imposition of translational symmetry in the inhomogeneous coordinate, x, implies that the larger plasma consists of an infinite array of identical plasma slabs (see, e.g., the model of Gerver *et al.* [7]). This is inappropriate because we are interested in the behavior of an isolated plasma slab. Also, because the physics allows qualitatively similar phenomena on both left and right sides of the plasma slab, we may avoid duplication of the physics and gain a factor of 2 in the simulation volume by imposing a symmetry on the larger plasma that incorporates this similarity.

The equilibrium plasma is taken to be an isolated plasma slab characterized by a number density, n_0, and a magnetic field, $\mathbf{B}_0$, that are functions of x only. n_0, a scalar, and $\mathbf{B}_0$, a pseudo-vector [8, 9] are required to be continuous across the simulation boundary. An appropriate boundary condition that meets these requirements may be obtained by demanding that the larger plasma be invariant under inversion through a point lying on the boundary of the simulation volume.

The inversion point is chosen, for convenience, to be the origin of the coordinate system. A particle that leaves the simulation volume at $(0, y)$ with a velocity, $\mathbf{v}$, will then be replaced by an image particle entering the simulation volume at $(0, -y)$ with a velocity $-\mathbf{v}$. This method of treating the particle boundary crossings lets both the computer particles and their images execute correct orbits in the given fields. Therefore there can be no nonphysical effects associated with these boundary crossings. Similarly, the boundary condition for the scalar potential, ϕ, is

$$\phi(x, y) = \phi(-x, -y), \tag{1}$$

which closes the finite difference representation of Poisson's equation at $x = 0$.

These boundary conditions have, as yet, been implemented only in electrostatic particle simulation codes. However, we expect that inversion boundary conditions will be particularly useful for bounded electromagnetic particle simulation models because there are no sudden changes in the orbits of particles at the boundary which might result in the emission of electromagnetic waves (bremsstrahlung). In an electromagnetic code utilizing inversion symmetry the boundary condition at $x = 0$ on the vector potential, $\mathbf{A}$, is

$$\mathbf{A}(x, y) = -\mathbf{A}(-x, -y). \tag{2}$$

Alternatively, using the electric field, $\mathbf{E}$, and the magnetic field, $\mathbf{B}$, directly, the finite difference version of Maxwell's equations may be closed at $x = 0$ by using

$$\mathbf{E}(x, y) = -\mathbf{E}(-x, -y) \tag{3}$$

and

$$\mathbf{B}(x, y) = \mathbf{B}(-x, -y). \tag{4}$$

Next a boundary condition at $x = LX$ needs to be specified. We note first that if inversion symmetry is used on this boundary (as well as on the boundary at $x = 0$), the result will be equivalent to a periodic system with boundaries at $-LX$ and LX; this is not our object. Instead, we have chosen to employ an "open-sided" boundary [10, 11] in which particles are reflected at $x = LX$, while the potential is matched with the spatially decaying vacuum solution for $x > LX$.

We note that the simulation model described here may be employed in simulating both neutral and nonneutral plasmas; for nonneutral plasmas the electric field is matched to the vacuum fields $E_x = \pm Q_{\text{total}}/2L_y$ at $x = \pm\infty$.

III. Two-Dimensional Simulation with the Inversion Symmetry

We have tested the inversion symmetry boundary condition in a two-dimensional particle simulation code. The code follows the dynamics of both electrons and ions in a uniform magnetic field using the well-known leap-frog scheme. We chose a

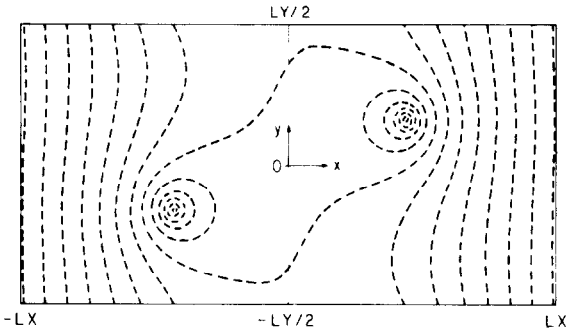

FIG. 2. Contours of potentials created by a single particle in the simulation volume. The potential satisfies $\phi(x, y) = \phi(-x, -y)$ and $\phi(x \to \infty, y) = 0$. The contours for $x < 0$ were obtained by inverting those for $x > 0$ about the origin (0, 0).

homogeneous plasma to test the code, even though the primary motivation for the use of the inversion symmetry is the simulation of inhomogeneous plasmas.

A counter plot of the potential created by a single particle in the system is shown in Fig. 2; the simulation volume is the $x > 0$ region of the x–y plane with the inversion symmetry boundary at $x = 0$ and the open boundary on the right. The potential is due to the particle and its inversion image particle in the region $x < 0$. The contours for $x < 0$ are obtained by inverting the potential in the simulation

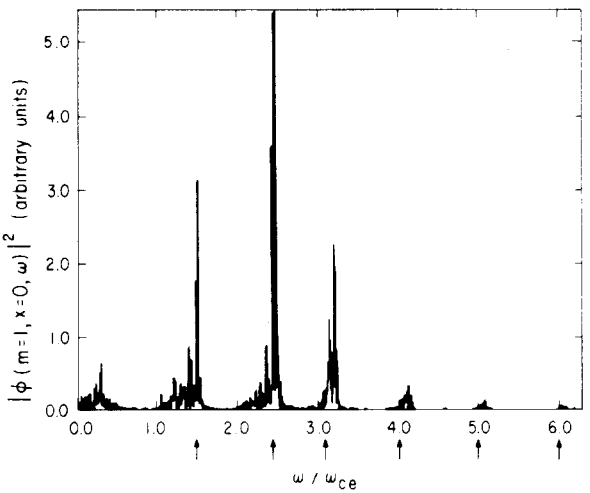

FIG. 3. The high-frequency power spectrum showing the electron Bernstein modes for the $m = 1$ Fourier mode ($k_y = 2\pi m/LY$) at $x = 0$ for time $0 \leqslant \omega_{pe} t \leqslant 4000$. The arrows along the horizontal axis indicates the frequencies for $k_\perp \rho_e \simeq 0.8$ obtained from the dispersion relation. Simulation parameters are 32×32 cells, 16,384 particles for each species, mass ratio $m_i/m_e = 25$, temperature ratio $T_e/T_i = 4$, electron cyclotron frequency $\omega_{ce} = 0.5$, electron Larmor radius $\rho_e = 4$, electron Debye length $\lambda_{De} = 2$, and time step $\Delta t = 0.25$, where electron plasma frequency ω_{pe} and grid size Δx are taken to be unity.

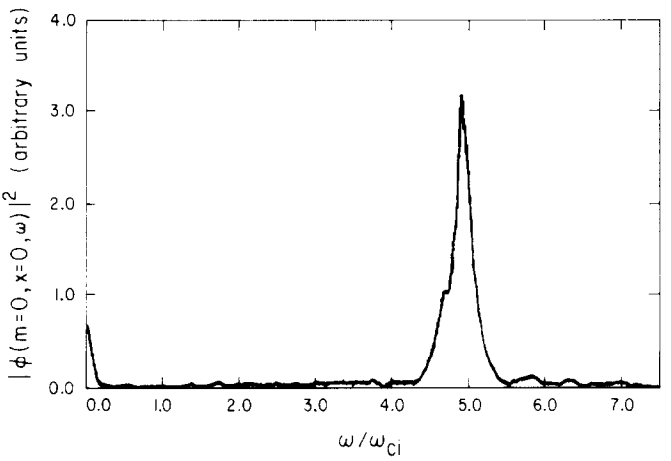

FIG. 4. The low-frequency spectrum for the $m = 0$ mode ($k_y = 0$) at $x = 0$ for time $0 \leqslant \omega_{pe} t \leqslant 4000$. The peak corresponds to the lower hybrid wave.

volume. The system shown is inversion symmetric about the point (0, 0). It is also inversion symmetric about the points $(0, \pm LY/2)$ because inversion through $(0, \pm LY/2)$ is just the product of inversion through (0, 0) and translation of $\pm LY$. The potential is seen to satisfy the boundary conditions imposed.

The system is loaded initially with a spatially homogeneous thermal plasma out to $x = LX$. The particles are reflected at $x = LX$. Two interesting results are the high- and low-frequency power spectra.

The high-frequency power spectrum is shown in Fig. 3 for the first Fourier mode

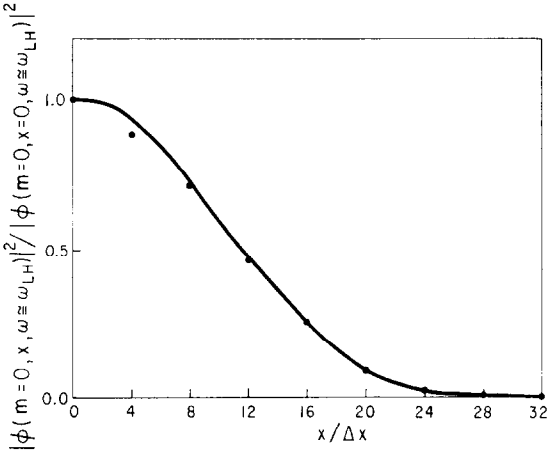

FIG. 5. Potential $|\phi(x)|^2$ mode structure for $m = 0$ and $\omega \simeq \omega_{LH}$. Dots are the simulation results and the solid line is the analytical result.

($k_y = 2\pi/LY$) at $x = 0$. Electron Bernstein modes are clearly in agreement with the expected frequencies for $k_\perp = k_y$ as indicated on the axis. Low-frequency peaks ($\omega < \omega_{ce}$, ω_{ce} = electron cyclotron frequency) due to the ions (such as ion Bernstein modes, and lower hybrid modes) are also seen.

The low-frequency power spectrum of the $k_y = 0$ mode at $x = 0$ is shown in Fig. 4. The peak at $\omega/\omega_{ci} \simeq 4.9$ is close to the lower hybrid frequency $\omega_{LH} \simeq \omega_{pi}/(1 + \omega_{pe}^2/\omega_{ce}^2)^{1/2} = 4.47\omega_{ci}$; the discrepancy is accounted for by the thermal effects. The spatial structure, $|\phi(x)|^2$, for this mode, $\omega \simeq \omega_{LH}$, can be obtained from power spectra of the potential at various points in x, as shown by the dots in Fig. 5. The dots compare well with the analytical result [12] shown by the solid line.

The simulation plasma under the inversion and open boundary conditions behaves as expected without any ill effects near either boundary. The homogeneous density profile was found to be maintained without abnormal behavior near $x = 0$ up to 16,000 time steps, with less than 3 % increase in the total system energy.

IV. Concluding Remarks

Inversion symmetry boundary conditions have been proposed for plasma simulations as an attractive alternative to other currently used boundary conditions [5, 6]. Initial test results of a two-dimensional particle code with an inversion symmetry boundary were found to be in agreement with theory.

We have used this modeling for drift cyclotron instability [13] and lower hybrid heatiung studies [14], with nonuniform densities, with good success, gaining the savings of a factor of 2 in computer time and storage. In addition, further savings have been gained using a guiding center particle mover for the electrons, in simulating low-frequency instabilities.

Acknowledgments

We are indebted to C. K. Birdsall for discussions and encouragement; the initial idea was suggested by one of us (MJG) in one of Professor Birdsall's seminars. We wish to thank A. B. Langdon and B. Lasinski for making their electromagnetic code, ZOHAR, available for us to convert to an electrostatic code with the inversion symmetry, called EZOHAR, and for their advice and support.

This work was supported by Department of Energy Grant EY-76-S-03-0034-PA128.

References

1. Y. Matsuda and H. Okuda, *Phys. Rev. Lett.* **36** (1976), 474.
2. W. W. Lee, Y. Y. Kuo, and H. Okuda, *Phys. Fluids* **21** (1978), 617.
3. A. T. Lin, *Phys. Fluids* **21** (1978), 1026.
4. C. Winske and D. W. Hewett, *Phys. Rev. Lett.* **35** (1975), 937.
5. W. W. Lee and H. Okuda, *J. Comput. Phys.* **26** (1978), 139.
6. H. Naitou, S. Tokuda, and T. Kamimura, *J. Comput. Phys.* **33** (1979), 86.

7. M. J. GERVER, C. K. BIRDSALL, A. B. LANGDON, AND D. FUSS, *Phys. Fluids* **20** (1977), 291.
8. H. GOLDSTEIN, "Classical Mechanics," p. 130, Addison–Wesley, Reading, Mass., 1950.
9. P. M. MOORE AND H. FESHBACH, "Methods of Theoretical Physics," Vol. I, p. 10, McGraw–Hill, New York, 1953.
10. O. BUNEMAN, *J. Comput. Phys.* **12** (1973), 124.
11. A. B. LANGDON AND B. LASINSKI, "Methods in Computational Physics" (B. Alder, S. Fernbach, and M. Rotenberg, Eds.), Vol. 16, p. 327, Academic Press, New York, 1976.
12. Y. MATSUDA AND W. M. NEVINS, to be submitted for publication.
13. Y. MATSUDA, *Bull. Amer. Phys. Soc.* **23** (1978), 825.
14. K. MATSUDA, Y. MATSUDA, AND G. E. GUEST, *Phys. Fluids* **23** (1980), 1422.

RECEIVED: June 19, 1979; REVISED: December 17, 1979

W. M. NEVINS,* Y. MATSUDA* AND M. J. GERVER†
Electronics Research Laboratory
University of California, Berkeley, California 94720

* Present address: Lawrence Livermore Laboratory, University of California, Livermore, CA 94550.
† Present address: Plasma Fusion Center, Massachusetts Institute of Technology, Cambridge, MA 02139.